ELSEVIER

International Journal of Pharmaceutics 122 (1995) 35–47

international journal of pharmaceutics

The effect of particle size and shape on the surface specific dissolution rate of microsized practically insoluble drugs

Mitra Mosharraf, Christer Nyström *

Department of Pharmacy, Pharmaceutics, Uppsala Biomedical Centre, Uppsala University, Box 580, S-751 23 Uppsala, Sweden

Received 6 May 1994; revised 12 January 1995; accepted 24 January 1995

Abstract

The effects of both particle shape and size on the dissolution rate of sparingly soluble micro-particles have been studied. Griseofulvin, three different qualities of barium sulphate, oxazepam and glibenclamide were chosen as the model substances. As these materials differed in both particle size (from 1.8 to 3.8 μm) and particle shape (from rounded, isodiametric to flaky or irregular particles), different combinations of particle size and shape were used to investigate their combined effect on the dissolution rate. The surface specific dissolution rate was determined, using a Coulter counter technique. The ratio of this value to the equilibrium solubility was calculated for all materials and its relation to the shape and size of the micro-particles was investigated. The results obtained indicated that the dissolution rates of sparingly soluble drugs are related to the particle shape as well as to the particle size. For particles of the same size, the dissolution rate decreased as the level of flakiness and irregularity increased. This phenomenon can be explained by an increase in the average hydrodynamic boundary layer thickness as the particles become more irregular. Therefore, the product of the surface shape factor and mean particle diameter was used to discuss the combined effect of these factors on the dissolution rates of sparingly soluble drugs.

Keywords: Particle shape effect; Particle size effect; Dissolution rate, surface specific

1. Introduction

1.1. General dissolution parameters

The dissolution rate of a drug is of special importance when it is the rate-limiting step for the uptake of drugs after oral administration. This is the case for many hydrophobic drugs with extremely low aqueous solubility (Anderberg, 1992). Therefore, investigation of different ways to enhance the dissolution of these drugs is of interest.

Dissolution of a solid dispersed in a liquid takes place in two stages. The first stage is an interfacial reaction between the solid phase and the liquid phase, which results in the liberation of solute molecules from the solid phase (i.e., solvation). The second stage is the transport of these molecules from the interface into the bulk medium under the influence of diffusion or convection.

The dissolution rate is thus determined by the rate of the slowest stage. In the absence of a

* Corresponding author.

SSDI 0378-5173(95)00033-X

chemical reaction between solute and solvent, the rate-limiting step is usually the diffusion process (Nogami et al., 1966; Carstensen, 1972) and the overall process is said to be diffusion-controlled. Investigation of diffusional transport in dissolution of suspended, practically insoluble drugs (Bisrat et al., 1992) showed that even for extremely sparingly soluble materials, the dissolution rate was diffusion-controlled. Noyes and Whitney (1897) and Nernst (1904) described the dissolution rate of the drug in a diffusion-controlled process by Eq. 1:

$$\frac{dc}{dt} = \frac{D}{Vh_D} S_c(C_s - C_t) \quad (1)$$

where dc/dt represents the dissolution rate, D is the diffusion coefficient of the solute, h_D denotes the thickness of the diffusion boundary layer, V is the volume of the dissolution medium and S_c represents the interfacial surface area, i.e., the surface area of the undissolved solid in contact with solvent.

C_s is the concentration of the solute required to saturate the solvent (i.e., equilibrium solubility) and C_t denotes the concentration of the solute in the bulk medium at time t.

If $C_t \ll C_s$ then the dissolution rate will be directly proportional to the saturated concentration (i.e., solubility) and Eq. 1 may be simplified to:

$$\frac{dc}{dt} = KS_cC_s \quad (2)$$

where K is equal to D/Vh_D. These circumstances are normally called 'sink conditions' and occur when the concentration of solute does not exceed 10% of the amount needed for equilibrium saturation. This situation is possible when the solute is removed from the medium at a faster rate than it passes into solution, or when the volume of the medium is very large.

Sink conditions may arise in vivo when a drug is absorbed from its solution in the gastrointestinal fluids faster than it dissolves in those fluids. This is one of the reasons for having sink conditions during the measurement of dissolution rate. The other reason is that under sink conditions, the dissolution rate will be directly proportional to the equilibrium solubility and the interfacial surface area.

1.2. Surface specific dissolution rate

It is often preferable that the dissolution rate is expressed in terms of a surface specific value (e.g., in μg/min per cm^2). This can be achieved either by exposing a constant surface area of the solid to the dissolving liquid or by continuously calculating or monitoring the change in surface area, as a function of time. The surface specific dissolution rate is often denoted by G in the literature, and is sometimes also referred to as the intrinsic dissolution rate. According to Nyström et al. (1985b), it is possible to calculate the surface specific dissolution rate for specific time intervals during the dissolution process, using a Coulter counter technique, where several physical parameters of the undissolved particle fraction are characterized. The procedure used was to calculate the surface area remaining (cm^2) and the weight dissolved (μg) as a function of time (min).

$$G = \frac{W_o - W_t}{t((S_o + S_t)/2)} \quad (3)$$

where W_o is the initial weight of solid particles and W_t represents the weight at time t, while S_o and S_t are the surface areas at the respective times.

An important assumption is that the particle shape remains constant during the dissolution process (Carstensen, 1980).

1.3. Calculation of the maximum surface specific dissolution rate

Nicklasson and Brodin (1984) postulated the possibility of calculating the maximum dissolution rate of a material from the following equation:

$$\log C_s = \log G + 1.94 \quad (4)$$

where C_s was described as the equilibrium solubility in mg/ml and G as the maximum dissolution rate in mg/s cm^2.

Their concept is based on the assumption, mentioned above, that the dissolution rate is diffusion controlled. By performing experiments at increasing rotational speeds for a rotating disc they suggested Eq. 4 was valid for a situation where the diffusional transport could be neglected, i.e., reflecting the maximum dissolution rate. In this study maximum values of G and G/C_s have been calculated according to Eq. 4, subsequently recalculated to the same units as presented in Eq. 3 and used as references to compare with experimental data obtained.

1.4. Effect of particle size on dissolution rate

According to Eq. 1 the dissolution rate is directly proportional to the interfacial surface area. Therefore, a decrease in particle size will result in an increase in dissolution rate. However, it has been shown (e.g., Bisrat and Nyström, 1988) that a decrease in particle size results in a higher increase in dissolution rate than can be explained solely by the increase in surface area. In dispersed solid-liquid systems, particle size reduction seems to result in an increase of the dissolution rate of a sparingly soluble material by decreasing the thickness of the diffusion layer around each particle (Niebergall et al., 1963; Bisrat and Nyström, 1988), and also by exhibiting a large interfacial surface area. (Noyes and Whitney, 1897; Brunner, 1904; Nernst, 1904). As the fraction of the hydrodynamic boundary layer thickness (h_H) in which diffusion dominates constitutes the diffusion boundary layer thickness (h_D), Bisrat and Nyström (1988) used the Prandtl boundary layer equation (Niebergall et al., 1963) to explain the effect of hydrodynamic boundary layer thickness on the dissolution rate of sparingly soluble materials.

According to the Prandtl boundary layer equation for flow passing a flat surface, the hydrodynamic boundary layer thickness (h_H) can be expressed as follows:

$$h_H = k(L^{1/2}/V^{1/2}) \quad (5)$$

where L is the length of the surface in the direction of flow, k denotes a constant and V is the relative velocity of the flowing liquid against the flat surface.

It is believed that a difference in particle diameter could correspond to a difference in the parameter L in Eq. 5. Bisrat and Nyström (1988) have shown that, for solids dispersed in a liquid medium under agitation, a decrease in particle size probably leads to a decrease in both L and V. Although these two parameters counteract each other, it was shown that the net effect was a thinner hydrodynamic layer around particles and an increase in the surface specific dissolution rate.

This phenomenon is especially pronounced for materials which have a mean particle size less than 5 μm (Anderberg et al., 1988; Bisrat and Nyström, 1988). However, so far relatively few results have been reported for materials finer than 5 μm and especially for materials finer than 3 μm.

It seems thus of interest to collect further data for such very fine particulate materials. As the effect of particle size on the effective diffusional distance is related to hydrodynamic mechanisms, it seems also to be of interest to evaluate the effect of particle shape in this context.

The aim of the present study was thus to examine the effect of both particle size and particle shape on surface specific dissolution rate for materials with an extremely low solubility and a mean particle size less than 5 μm.

2. Materials and methods

2.1. Test materials

2.1.1. Griseofulvin

The griseofulvin (Glaxo, UK) used in the present study has been well characterized in an earlier investigation (Anderberg and Nyström, 1990) and is used here as a reference.

2.1.2. Barium sulphate

In this study three different qualities of barium sulphate were studied. They will be referred to as quality I, II (Kebo, Sweden), and III. Quality III was obtained by milling quality II at our labora-

tory using a Mortar grinder (Mortar grinder, type KMI, Germany).

2.1.3. Glibenclamide

Glibenclamide (Hoechst, Germany) was used as supplied.

2.1.4. Oxazepam

Oxazepam (Kabi Pharmacia, Sweden) oxazepam was milled using a pin disc mill (Alpine 63 C, Germany) and then classified in an air classifier (Alpine 100 MZR, Alpine AG, Germany) in which the fractions smaller than 2 μm were separated.

2.2. Electrolyte medium

To be able to use a Coulter counter the medium must be an electrolyte. This was achieved by adding 0.9% w/w NaCl to a specific volume of de-ionised particle-free water. In order to improve the wettability of the powders, 0.01% w/w polysorbate (Tween 80) was also added to the electrolyte.

2.3. Sample preparation

A stock suspension of a known concentration was prepared by dispersing the powder samples in particle-free electrolyte. The suspension was subjected to ultrasonic agitation for a period of 10 min to break up any particle agglomerates. A certain volume of the suspension was added to a known volume of medium depending on the purpose of the experiment. Stock suspensions were used in particle size analysis, estimation of particle shape by scanning electron microscopy, solubility and dissolution rate studies.

2.4. Particle size analysis

This experiment was carried out using an electrical sensing zone method (Coulter counter Model TA II). The Coulter counter was fitted with an aperture tube of 30 μm.

A certain volume of the stock suspension was added to 200 ml particle-free medium and the number of particles in 14 size classes was recorded. The amount of stock suspension added to the medium was chosen so that its final amount should not result in a coincidence error greater than 2–3%. Knowing the number of particles in each size class, the mean particle size and the particle size distribution were determined for all test materials (Nyström et al., 1985a).

To reduce the dissolution of barium sulphate particles, an electrolyte medium saturated with barium sulphate was used.

2.5. Measurement of density

The apparent particle density of each compound was measured by an air comparison pycnometer (Beckman Model 930, USA).

2.6. Measurement of external surface area

The external specific surface area was determined, under both fixed and variable pressure, by different permeametric methods.

2.6.1. Measurements at fixed pressure

A Fisher sub-sieve sizer apparatus was used to maintain the measurements at constant pressure. The calculation of surface area according to this method, does not include a correction for 'slip flow' (Alderborn et al., 1985).

2.6.2. Measurements at variable pressure

A Blaine apparatus (Blaine, 1943) was used for measurements at variable pressure. The results obtained from these experiments were corrected for slip flow (Alderborn et al., 1985). This means that the calculations involved terms for both viscous and molecular flow, so that this method provided a better estimate of the external surface area.

2.7. Measurement of total surface area

The total surface area was measured by the gas adsorption, BET method (Flowsorb II 2300). In this test nitrogen gas was used.

2.8. Estimation of particle shape

The particle shape of the test materials was determined by the following two methods.

2.8.1. Scanning electron microscopy

In order to estimate the particle shape of the test materials, a suspension of each sample was prepared as described above. A certain volume of each suspension was then filtered through a polycarbonate filter (Nuclepore 13 mm, 0.2 μm). These specimens were then characterized by scanning electron microscopy.

2.8.2. Quantitative determination

The following equation, which relates particle diameter and volume specific surface area to particle shape, was used for calculating the surface to volume shape factor (Heywood, 1954):

$$S_v = \frac{\alpha_{sv}}{d_{sv}} \quad (6)$$

where S_v is the volume specific surface area in cm^2/cm^3, d_{sv} denotes the volume specific mean particle diameter in cm and α_{sv} is the surface to volume shape factor (Heywood's shape factor). The minimum value for this shape factor equals 6, which refers to spherical particles. The value increases for particles that deviate from the spherical.

The surface to volume shape factors were calculated for all test materials. The volume specific surface areas, used for this purpose, were based on the results obtained from the Blaine apparatus (Table 2). d_{sv} was assumed to be equal to the harmonic mean diameter by weight (d_{wh}) according to Herdan, 1960. It was calculated from the Coulter counter data and is listed in Table 1.

Knowing the surface to volume shape factors, the surface shape factors (α_s) were also calculated using the following equation:

$$\alpha_s = \alpha_{sv}\pi/6 \quad (7)$$

2.9. Determination of aqueous solubility and the surface specific dissolution rate

These experiments were carried out using a Coulter counter technique (Nyström et al., 1985a,b) as described below.

2.9.1. Solubility determination

A certain volume of the stock suspension was added to a known volume of particle free medium so that the initial amount of particles present in

Table 1
Primary characteristics of the test materials

Material	Particle size distribution by weight			Density [a] (g/cm^3)	Surface area (m^2/g)			Surface shape factor [b] α_s (–)
	d_{wg} [c] (μm)	∂_g [d] (–)	d_{wh} [e] (μm)		External		Total BET	
					Blaine [f]	Fisher [g]		
Griseofulvin	3.70	1.76	3.13	–	1.94	1.57	–	4.6
Griseofulvin [h]	3.10	1.50	–	1.44	2.10	–	–	4.4
Glibenclamide	1.84	1.82	1.57	1.37	4.50	2.41	–	5.1
Barium sulphate I	1.77	1.49	1.61	4.57	2.63	1.54	3.13	10.2
Barium sulphate II	3.36	1.34	3.13	4.56	2.32	1.60	2.55	17.3
Barium sulphate III	2.03	1.41	1.89	4.56 [i]	2.39	–	–	10.8
Oxazepam	3.99	1.57	3.51	1.48 [j]	4.05	2.66	5.63	11.0

[a] Measured by a Beckman pycnometer.
[b] Calculated according to Eq. 6 and 7.
[c] Geometric mean volume diameter by weight.
[d] Geometric standard deviation.
[e] Harmonic mean volume diameter by weight.
[f] Variable pressure.
[g] Fixed pressure.
[h] Earlier reported data (Anderberg and Nyström, 1990).
[i] Was assumed to be equal to the density of barium sulphate quality II.
[j] According to an earlier study (Westerberg and Nyström, 1993).

the medium would exceed the amount required for a saturated solution. These initial amounts were in the concentration range of 10–12 μg/ml. The number of particles was then recorded in 14 size classes as a function of time until an equilibrium was reached (i.e., a saturated solution was obtained). All the measurements were carried out at room temperature (22 ± 1° C).

The equilibrium solubility was then calculated by subtracting the remaining amount of sample present in the medium at the time of saturation from the initially characterized amount (Nyström et al., 1985a,b; Nyström and Bisrat, 1986; Anderberg et al., 1988).

2.9.2. Surface specific dissolution rate

In order to determine the surface specific dissolution rate of the materials, a certain amount of the stock suspension was added to 300 ml particle-free medium to provide sink conditions. The concentration of the substance in the dissolution medium at the starting time of dissolution process was thus equal to 0.5 μg/ml in all cases except that of oxazepam where a concentration of about 2 μg/ml was required to maintain sink conditions.

These measurements were carried out in a flat-bottom beaker with an outside diameter of 75 mm and a height of 96 mm. Water depth (i.e., the height of the fluid surface from the bottom of beaker when filled with 300 ml particle-free medium at 22 ± 1° C) was 64 mm and the Coulter orifice was centered at a distance of 27 mm from the bottom of the beaker.

Agitation was produced using a standard twin-blade Coulter counter impeller. During the experiment the total volume of medium, the agitation intensities and temperature were kept constant at 300 ml, 877 rpm and 22° C, respectively.

The number of particles per min, in 14 size classes was recorded, until 85% of all material was dissolved. This process took about 5–15 min depending on the characterized material.

From the size distribution data the surface specific dissolution rate was calculated according to Eq. 2.

3. Results and discussion

3.1. Particle size analysis

All test materials in this study had a log-normal size distribution. Thus, the mean particle size was defined as the geometric mean volume diameter by weight (d_{wg}) and subsequently a geometric standard deviation (∂_g) was used (Table 1).

As shown in Table 1, all the test materials used in the present study had a geometric mean volume diameter smaller than 4 μm. Barium sulphate quality I and glibenclamide were the finest materials with a mean particle size of 1.77 and

Table 2
Surface specific dissolution rate and solubility data

Material	Intrinsic dissolution rate (G) (μg/min per cm^2)		Aqueous solubility (C_s) (μg/ml)	G/C_s	
	Theoretical maximum value [a]	Experimental data [b]		Theoretical maximum value [a]	Experimental data [b]
Griseofulvin	5.6	13.7	8.1	0.69	1.69
Griseofulvin [c]	4.8	11.2	7.0 [c]	0.69	1.60 [c]
Glibenclamide	4.1	14.0	5.9	0.69	2.35
Barium sulphate I	4.3	10.3	6.3	0.69	1.63
Barium sulphate II	4.3	3.4	6.3	0.69	0.53
Barium sulphate III	4.1	5.5	5.9	0.69	0.84
Oxazepam	16.0	9.9	23.3 [d]	0.69	0.42

[a] Calculated according to Eq. 4.
[b] Calculated according to Eq. 3.
[c] Earlier reported data (Anderberg and Nyström, 1990).
[d] According to an earlier study (Westerberg and Nyström, 1993).

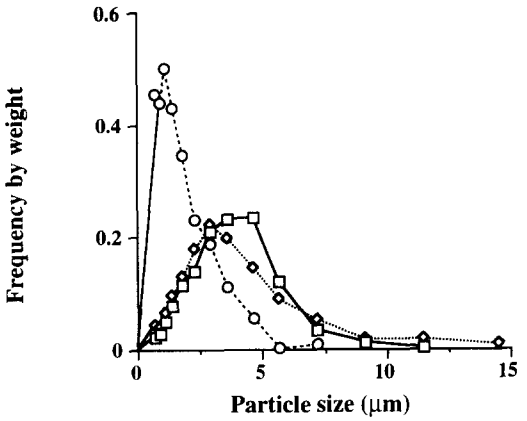

Fig. 1. Particle size distribution of griseofulvin, oxazepam and glibenclamide characterized by the Coulter counter TA II. (◇) Griseofulvin, (□) oxazepam, (○) glibenclamide.

1.84 μm. Oxazepam, griseofulvin and barium sulphate quality II had a mean particle size of 3.99, 3.70 and 3.36 μm, respectively. Finally, barium sulphate quality III which was obtained by milling the barium sulphate quality II had a mean particle diameter of 2.03 μm.

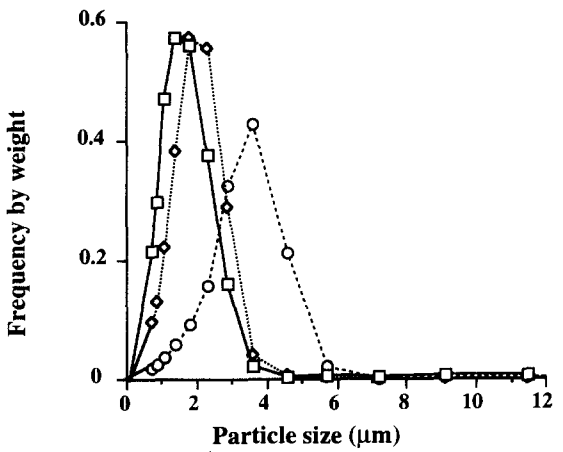

Fig. 2. Particle size distribution of barium sulphate quality I–III. (□) Barium sulphate quality I, (○) barium sulphate quality II, (◇) barium sulphate quality III.

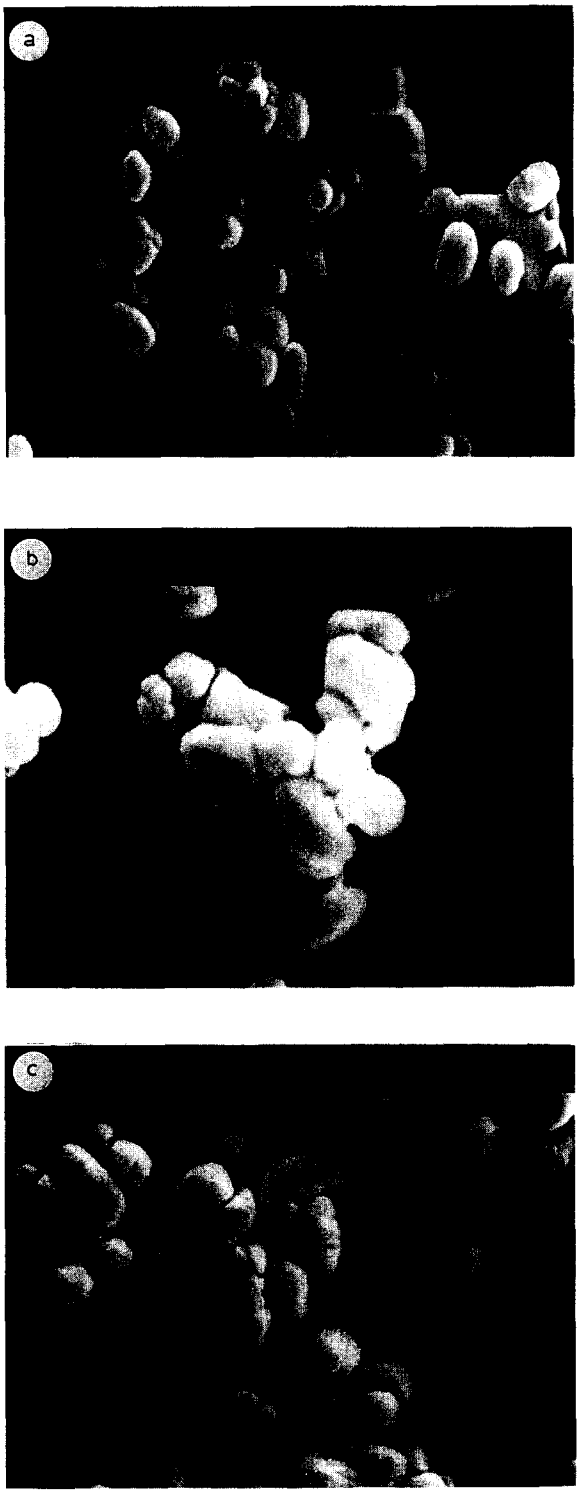

Fig. 3. Scanning electron photomicrograph of barium sulphate. (a) Barium sulphate quality I, (b) barium sulphate quality II, (c) barium sulphate quality III.

Considering the size distribution profiles (Fig. 1 and 2) it can be concluded that the 30 μm capillary tube covers almost the entire particle size range of all the materials. However, in the case of glibenclamide some particles smaller than 0.6 μm were found, which were outside the covering range of the capillary tube. However, they represented a very limited fraction by weight.

3.2. Density

The results are the mean values of three determinations and are presented in Table 1.

3.3. Surface area and particle shape analysis

The external and total surface areas of the test materials are presented in Table 2. All results are the average of three determinations.

In order to estimate the shape variations of the test materials, both surface shape factors (α_s) and surface to volume shape factors (α_{sv}) (Table 2) were calculated as described above (Eq. 6 and 7). The minimum possible value for α_s is π (i.e., 3.14) and for α_{sv} it is equal to 6 which refers to a sphere. When particles deviate from sphericity and become more asymmetrical, larger values are found for α_s and α_{sv}.

Considering the values listed in Table 2, it can be concluded that both griseofulvin and glibenclamide particles had the smallest deviation from a spherical shape while the barium sulphate qualities, especially barium sulphate quality II, seemed to be very flaky or irregular.

These results correlate relatively well with the electron photomicrographs (Fig. 3 and 4). However, as can be seen in the electron photomicrograph of barium sulphate quality II (Fig. 3), the particles consist of strongly fused aggregates which are not broken to primary particles even after an ultrasonic treatment of 10 min duration. Therefore, it was assumed that these strongly

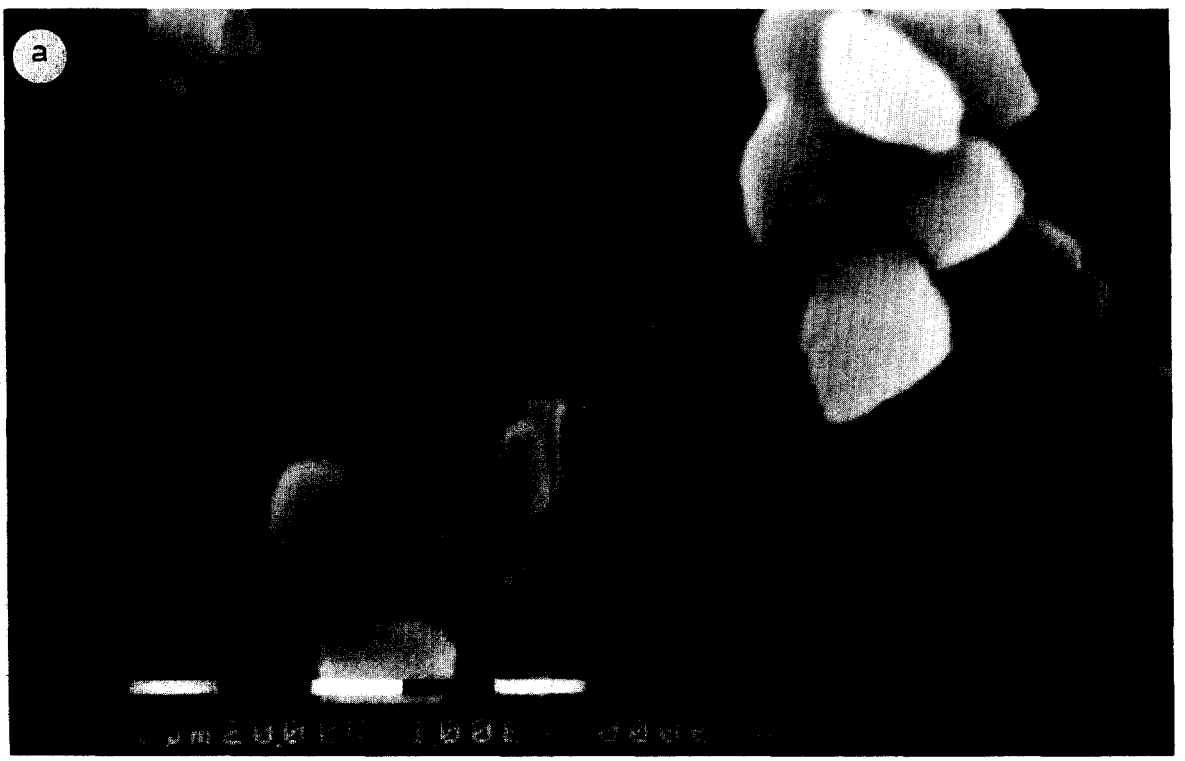

Fig. 4. Scanning electron photomicrograph of griseofulvin, glibenclamide and oxazepam. (a) Griseofulvin, (b) glibenclamide, (c) oxazepam.

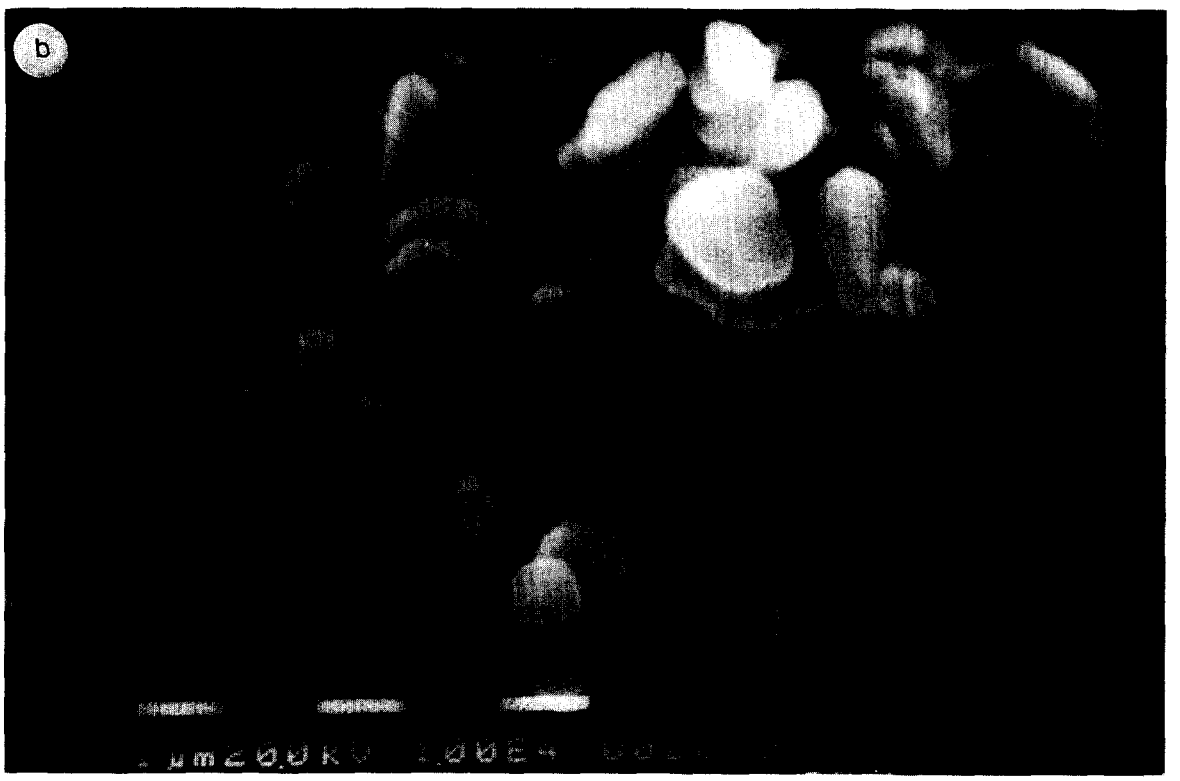

Fig. 4 (continued).

fused particles behaved as the primary particles which took part in the dissolution process.

In the case of glibenclamide and griseofulvin, the electron photomicrographs showed that the particles were almost of the same shape, even though the glibenclamide particles were only half

the size of the griseofulvin particles. Oxazepam particles, on the other hand, were quite flaky with a rough and irregular surface texture (Fig. 4).

3.4. Solubility and surface specific dissolution rate

The solubility values are presented in Table 2 and are mean values of three determinations (except the result for barium sulphate quality III, which is based on a single determination). In the case of oxazepam the solubility value refers to an earlier study (Westerberg and Nyström, 1993) based on photometric analysis.

Both theoretical maximum values and experimental G values were calculated. Maximum theoretical G values were calculated from Eq. 4, using the experimentally obtained solubility data. Experimental G values were obtained according to Eq. 3 and are the average of at least three determinations.

Different G values for test materials can probably be related to their differences in equilibrium solubility. Therefore, these values were also corrected for this parameter and compared to the maximum G/C_s values based on Eq. 4. These data are summarised in Table 2.

A comparison of the theoretical maximum surface specific dissolution rate with the data obtained from the present study and previous studies (Bisrat and Nyström, 1988; Anderberg and Nyström, 1990) shows that in some cases the experimental data are markedly greater than the maximum value suggested by Niklasson and Brodin (1984).

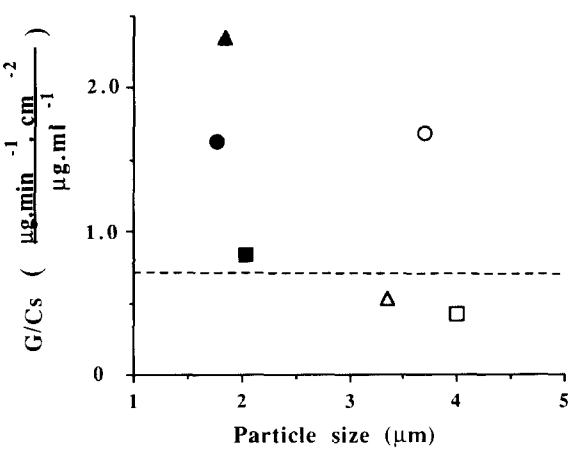

Fig. 5. Influence of particle size on the surface specific dissolution rate (G) corrected for the effect of solubility (C_s). The dotted line represents the maximum theoretical value of G/C_s suggested by Nicklasson and Brodin (1984) and calculated from Eq. 4. (○) Griseofulvin, (▲) glibenclamide, (●) barium sulphate quality I, (△) barium sulphate quality II, (■) barium sulphate quality III, (□) oxazepam.

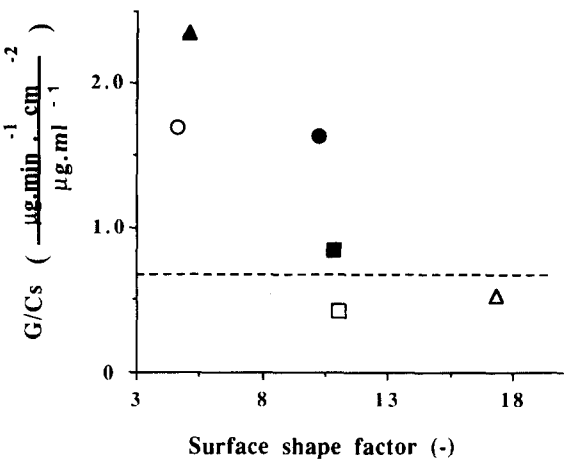

Fig. 6. Influence of particle shape on the surface specific dissolution rate (G) corrected for the effect of solubility (C_s). Symbols as in Fig. 5.

3.5. The effect of particle size on the surface specific dissolution rate

It should be kept in mind that the dissolution rates discussed in the present study are corrected for the effect of both solubility and surface area. Hence, according to an earlier study (Bisrat and Nyström, 1988) the differences in G/C_s values should correspond to differences in hydrodynamic boundary layer thickness around the particles, caused by particle size variations.

However, the results obtained indicate that in some cases particle size differences are not sufficient to explain the differences in surface specific dissolution rates.

For example, glibenclamide and barium sulphate quality I with mean particle sizes of 1.84 and 1.77 μm, respectively, should give the same G/C_s values. However, as is listed in Table 2, the actual values (2.35 and 1.63) were quite different.

Another comparison which can be made is between griseofulvin and barium sulphate quality

I. As listed in Table 1 these samples differed by about 2 μm in mean particle size. Thus, griseofulvin was expected to dissolve more slowly than barium sulphate quality I. However, comparing the G/C_s values listed in Table 2 and considering Fig. 5 it can be seen that they had almost the same G/C_s values (i.e., 1.69 and 1.63).

It thus seems that, in addition to the factors discussed so far, at least one other factor must be involved in the dissolution process.

3.6. The effect of particle shape on the surface specific dissolution rate

In order to investigate the influence of particle shape on the dissolution rate, G/C_s values were also plotted against shape factors in Fig. 6.

Considering glibenclamide, barium sulphate I and barium sulphate II, it seems that as the degree of shape irregularity (i.e., the value of α_s in this case) increases, the G/C_s value decreases. Some of the samples, though, tend to deviate from this. Glibenclamide and griseofulvin, with almost the same particle shapes and different G/C_s values exemplify these deviations. Other examples are barium sulphate quality I, quality II and oxazepam, which, with α_s values of 10.2, 10.8 and 11.0, respectively (i.e., almost the same particle shape), did not result in the same G/C_s values.

However, it seems that particle shape must be considered in interpreting the surface specific dissolution rate of a sparingly soluble material. The effect of particle shape seems to be especially pronounced for materials which deviate markedly from sphericity.

The mechanism of this observation may be explained by reference to the Prandtl boundary layer equation (Eq. 5). In the present study, it is suggested that long, flaky particles with a high degree of irregularity, may cause an increase in the average hydrodynamic boundary layer thickness, by increasing parameter L in Eq. 5.

3.7. The combined effect of particle size and shape on the surface specific dissolution rate

From a comparison of the G/C_s values of griseofulvin ($d_v = 3.70$ μm, $\alpha_s = 4.6$), and barium sulphate II ($d_v = 3.36$ μm, $\alpha_s = 17.3$), it can be concluded that particles with almost the same volume diameter, but unequal surface shape factors, will differ in surface specific dissolution rate.

On the other hand, if both particle size and shape factor increase, an increase in parameter L, and hence in the hydrodynamic boundary layer thickness, will be observed. If these two factors act together the net effect will be a remarkable decrease in the G/C_s value. This is true for barium sulphate II ($d_v = 3.36$ μm, $\alpha_s = 17.3$) and barium sulphate I ($d_v = 1.77$ μm, $\alpha_s = 10.2$).

If the particle size decreases in the same ratio that the shape factor increases, no remarkable differences in G/C_s values would be expected, since the two factors counteract each other. A comparison between griseofulvin and barium sulphate I exemplifies this. When both particle size and α_s decrease, (e.g., barium sulphate qualities II and III), a substantial increase in the G/C_s value occurs.

It is thus apparent that an increase in the surface shape factor together with an increase in particle size causes an increase in parameter L, resulting in an increase in the average hydrodynamic boundary layer thickness around the particles. Thus, this parameter must be considered as a relevant factor in both particle shape and particle size.

In order to study the net effect of size and shape on the surface specific dissolution rate, G/C_s values were plotted against the product of the geometric mean particle diameter by weight and the surface shape factor (i.e., '$d_v \times \alpha_s$') in Fig. 7. All the values fall on a single curve.

As illustrated in Fig. 7, it seems that for large irregular particles the dissolution rate is relatively low, while for small spherical particles the dissolution rate is relatively high.

4. Conclusion

The results of the present study seem to be in good agreement with earlier reported data (e.g., Grant et al., 1986), indicating that micronization does not always lead to a faster dissolution rate. The effect of particle shape on the dissolution

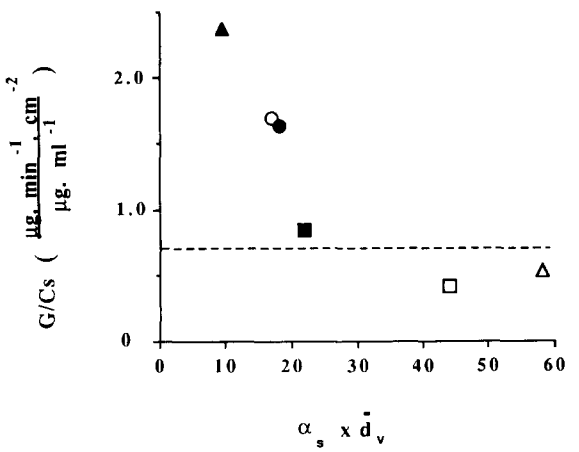

Fig. 7. Combined effect of particle size and shape on the surface specific dissolution rate (G) corrected for the effect of solubility (C_s). Symbols as in Fig. 5.

rate of sparingly soluble drugs has also been emphasised by other researchers (e.g., Chakrabarti et al., 1978). However, the reason for this observation has not always been elucidated and has often remained unclear.

In contrast to earlier studies, efforts have been made to discuss the combined effects of these two factors on the dissolution rate, from a hydrodynamic point of view. Particle shape is suggested to affect the surface specific dissolution rate by affecting parameter L in the Prandtl boundary layer equation and thereby resulting in a change in the average hydrodynamic boundary layer thickness. This leads to a change in the distance over which diffusion dominates and hence causes a change in the dissolution rate.

As has been suggested earlier (e.g., Nyström and Bisrat, 1986), the influence of particle size on the surface specific dissolution rate can be explained by this mechanism. Thus, the importance of geometrical form (i.e., size and shape) of the particles should be emphasized in all discussions that concern the dissolution rate of fine particulate sparingly soluble drugs.

The overall effect of size and shape was estimated by using the product of a mean particle size and a shape factor. However, there are certainly other ways of combining these two factors. Some authors (e.g., Farin and Avnir, 1992) have combined these two factors from a fractal geometrical point of view, but nobody has related their effect on dissolution rate to the hydrodynamics.

The results of the present study indicate that small spherical particles have a higher dissolution rate than large, irregular particles.

Finally, it should be mentioned that the maximum G/C_s value obtained experimentally in this study is much greater than the theoretical maximum value (Fig. 7 and Table 2) suggested by Nicklasson and Brodin (1984).

Acknowledgements

The authors wish to thank Glaxo, UK, Hoechst, Germany and Kabi Pharmacia, Sweden for supplying the griseofulvin, glibenclamide and oxazepam samples, respectively. The authors are also grateful to Mrs Elisabet Börjesson for skilful measurements of the total surface areas of the samples by the BET method, and also for her help in milling and classifying the oxazepam samples.

References

Alderborn, G., Duberg, M. and Nyström, C., Studies on direct compression of tablets: X. Measurement of tablet surface area by permeametry. *Powder. Technol.*, 41 (1985) 49–56.

Anderberg, E.K., Studies on the dissolution of fine particulate practically insoluble drugs and on the effect of surface active enhancers on gastrointestinal absorption of hydrophilic drugs. *Acta Univ. Ups. Comprehensive Summaries of Uppsala Dissertations from the Faculty of Pharmacy*, Reprocentralen, HSC, Uppsala, 1992, Vol. 91, p. 8.

Anderberg, E.K. and Nyström, C., Physicochemical aspects of drug release: X. Investigation of the applicability of the cube-root law for characterization of the dissolution rate of fine particulate materials. *Int. J. Pharm.*, 62 (1990) 143–151.

Anderberg, E.K., Nyström, C. and Bisrat, M., Physicochemical aspects of drug release: VII. The effect of surfactant concentration and drug particle size on solubility and dissolution rate of Felodipine, a sparingly soluble drug. *Int. J. Pharm.*, 47 (1988) 67–77.

Bisrat, M. and Nyström, C., Physicochemical aspects of drug release: VIII. The relation between particle size and surface specific dissolution rate in agitated suspensions. *Int. J. Pharm.*, 47 (1988) 223–231.

Bisrat, M. Anderberg, E.K., Barnett, M.I. and Nyström, C., Physicochemical aspects of drug release: XV. Investigation of diffusional transport in dissolution of suspended, sparingly soluble drugs. *Int. J. Pharm.*, 80 (1992) 191–120.

Blaine, R.L., A simplified air permeability fineness apparatus. *ASTM Bull.*, 123 (1943) 51–55.

Brunner, E., Theorie der Reaktionsgeschwindigkeit in heterogenen systemen. *Z. Phys. Chem.*, 47 (1904) 56–102.

Carstensen, J.T., *Solid Pharmaceutics: Mechanical Properties and Rate Phenomena*, Academic Press, London, 1980, p. 52.

Carstensen, J.T., *Theory of Pharmaceutical Systems*, Academic Press, New York, 1972, Vol. 1, pp. 238–241.

Chakrabarti, S., Van Severen, R. and Braeckman, P., Studies on the crystalline form of phenytoin. *Pharmazie*, 33 (1978) 338–339.

Farin, D. and Avnir, D., Use of fractal geometry to determine effects of surface morphology on drug dissolution. *J. Pharm. Sci.*, 81 (1992) 54–57.

Grant, D.J.W., Chow, K.Y. and Lam, S., Relationships between the solid state properties of griseofulvin obtained from different sources and crystallized under various conditions. *Proceedings of the 4th International Conference of Pharmaceutical Technology*, Paris, 1986, Vol. 1, pp. 23–32.

Herdan, G., *Small Particle Statistics*, 2nd Edn, Pitman Press, Bath, 1960, p. 35.

Heywood, H., Particle shape coefficients. *J. Imp. Coll. Chem. Eng. Soc.*, 8 (1954) 25–33.

Nernst, W., Theorie der Reaktionsgeschwindigkeit in heterogenen Systemen. *Z. Phys. Chem.*, 47 (1904) 52–55.

Niebergall, P.J., Milsovich, G. and Goyan, J.E., Dissolution rate studies: II. Dissolution of particles under conditions of rapid agitation. *J. Pharm. Sci.*, 52 (1963) 236–241.

Nicklasson, M., Brodin, A., The relation between intrinsic dissolution rates and solubilities in water-ethanol binary solvent system. *Int. J. Pharm.*, 18 (1984) 149–155.

Nogami, H., Nagai, T. and Sasuta, A., Powder preparations. XVII. Dissolution rate of sulfonamides by rotating disc method. *Chem. Pharm. Bull.*, 14 (1966) 329–338.

Noyes, A. and Whitney, W., The rate of solution of solid substances in their own solutions. *J. Am. Chem. Soc.*, 19 (1897) 930–934.

Nyström, C. and Bisrat, M., Coulter counter measurements of solubility and dissolution rate of sparingly soluble compounds using micellar solutions. *J. Pharm. Pharmacol.*, 38 (1986) 420–425.

Nyström, C., Barnett, M.I., Mazur, J. and Glazer, M., Determination of the solubility and dissolution rate of polydispersed materials from particle weight and surface area data using a TAII Coulter counter. *Proceedings of the 5th Conference on Particle Size Analysis*, Bradford, September, 1985b.

Nyström, C., Mazur, J., Barnett, M.I. and Glazer, M., Dissolution rate measurements of sparingly soluble compounds with the Coulter counter model TAII. *J. Pharm. Pharmacol.*, 37 (1985a) 217–221.

Westerberg, M. and Nyström, C., Physicochemical aspects of drug release: XVII. The effect of drug surface area coverage of carrier materials on drug dissolution from ordered mixtures. *Int. J. Pharm.*, 90 (1993) 1–17.